Argonne
NATIONAL LABORATORY

Implementation of the Flow Instability Model for the University of Missouri Reactor (MURR) That is Based on the Bernath Critical Heat Flux Correlation

Nuclear Engineering Division

Implementation of the Flow Instability Model for the University of Missouri Reactor (MURR) That is Based on the Bernath Critical Heat Flux Correlation

by
E.E. Feldman
Nuclear Engineering Division, Argonne National Laboratory

July 2011

TABLE OF CONTENTS

LIST OF FIGURES

LIST OF TABLES

IMPLEMENTATION OF THE FLOW INSTABILITY MODEL FOR THE UNIVERSITY OF MISSOURI REACTOR (MURR) THAT IS BASED ON THE BERNATH CRITICAL HEAT FLUX CORRELATION

Earl E. Feldman

Global Threat Reduction Initiative (GTRI) – Conversion Program
Nuclear Engineering Division
Argonne National Laboratory
9700 S. Cass Avenue
Argonne, Illinois 60439

ABSTRACT

A model that is based on the Bernath critical heat flux correlation and used to predict flow instability during steady-state operation of the University of Missouri Reactor (MURR) is described in detail. The model is evaluated via a computer spreadsheet, Table 8. The determination of key input data for the Table 8 model is demonstrated by a series of sample calculations shown in Tables 1 through 4. This model supersedes the model used in both References 2 and 3.

1 BACKGROUND

A key safety requirement of the University of Missouri Research Reactor (MURR) is that flow instability in the reactor core be avoided during steady-state operation. The MURR safety analysis uses the Bernath critical heat flux (CHF) correlation[1] to assess margin to flow instability.[2,3] A sufficient margin to flow instability is deemed demonstrated if the following two criteria are met: 1) the local heat flux at every location within the reactor core is no greater than half of the local value of critical heat flux based on the Bernath correlation and 2) there is no bulk boiling at the exit of any coolant channel. Except for conditions of very low flow rates and high coolant inlet temperatures, the first criterion is the more restrictive one.

A computer spreadsheet model based on the above criteria has been developed to determine the margin to flow instability for any MURR reactor core coolant channel. The purpose of this report is to describe the model and its implementation.

Another safety requirement of the MURR reactor is that an adequate margin to CHF is always maintained. The power at which the Bernath correlation predicts CHF to occur is always at least double the maximum reactor power allowed by the MURR flow instability criteria.

2 USE OF THE BERNATH CHF CORRELATION FOR THE MURR APPLICATION

The Bernath Correlation is given by:

$$(Q/A)_{BO} = h_{BO}\left(T_{w_{BO}} - T_b\right)$$

$$h_{BO} = 10890\left(\frac{D_e}{D_e + D_i}\right) + (\text{slope}) \, V$$

$$\text{slope} = 48/D_e^{0.6} \quad \text{if } D_e \leq 0.1 \, \text{ft} \tag{1}$$

$$\text{slope} = 90 + 10/D_e \quad \text{if } D_e > 0.1 \, \text{ft}$$

$$T_{w_{BO}} = 57 \ln P - 54\left(\frac{P}{P+15}\right) - \frac{V}{4}$$

where $(Q/A)_{BO}$ is the critical heat flux in p.c.u.[*] /hr-ft^2 (BO stands for "burnout"), h_{BO} is the heat transfer coefficient corresponding to the CHF in p.c.u./hr-ft^2-C, $T_{w_{BO}}$ is the wall temperature at which CHF occurs in °C, T_b is the local bulk coolant temperature in °C, D_e is the hydraulic diameter of the coolant passage in feet, defined as four times the channel flow area divided by the total wetted perimeter of the channel, D_i is the diameter of the heater surface in feet, defined by Bernath as the heated perimeter divided by π, P is the pressure in psia, and V is the velocity of the coolant in ft/s.

Equation (1) is a function that has five independent variables, T_b, D_e, D_i, V, and P and one dependent, or output variable, $(Q/A)_{BO}$, which is the local value of Bernath critical heat flux. In the case of the MURR reactor, D_i is the sum of the heated clad surface arc lengths of the one or two fuel plates that bound the channel divided by π. The other three quantities, T_b, V, and P vary along the length of the channel.

For normal operating conditions the pressure decreases from channel inlet to exit and is about 12 or 13 psia lower at the exit than at the inlet for a 3600 gpm flow rate. As was assumed in the 1974 analysis of the MURR reactor, [2,3] the pressure, P, at the exit will be conservatively assumed to apply to all axial levels. Using the exit pressure for all axial levels is a bounding assumption because critical heat flux increases with pressure in equation (1). Thus, only T_b and V are needed as functions of axial level. The axial distribution of T_b depends on the axial distribution of heat flux from the plates that bound the channel. Since the channel flow area does not vary with axial position, V is inversely proportional to coolant density. Because bulk boiling at the channel exit it not permitted, the bulk coolant temperature over the entire channel length is always subcooled, i.e., single-phase liquid. The relatively small variation of bulk coolant density with axial location is included in the model. A Visual Basic for Applications (VBA) program (or macro) was written to automatically execute the spreadsheet model for 60 combinations of input parameter values and record the 60 sets of results in spreadsheet tables for each pressurizer pressure.

---

[*] A p.c.u. is a "pound centigrade unit". 1 p.c.u. is equal to 1.8 Btu's.

In concept, at each axial level of each channel in the reactor core, for each heated surface the ratio of local heat flux to the Bernath CHF as defined by equation (1) would be determined for an assumed reactor power level and a specified set of the three independent variables, i.e., pressurizer pressure, core coolant flow rate, and coolant inlet temperature. Then by iteration, the assumed power level would be adjusted until the largest ratio of local heat flux to local Bernath CHF throughout the core is 0.5 or a coolant channel exit temperature reaches the saturation temperature. This would provide the maximum reactor power corresponding to the MURR Safety Limit Criteria for the three specified independent variables. In practice, a computer spreadsheet model was developed which considers only one reactor coolant channel at a time. Only the potentially limiting channels in the reactor were specifically analyzed with this model. The iteration on power level was performed automatically by the computer spreadsheet so that the desired maximum heat flux ratio of 0.499999 is achieved. Hot channel factors due to manufacturing tolerances and modeling uncertainties were included in the analysis. The safety envelope for MURR was obtained by determining the value of allowed reactor power for a range of values of pressurizer pressure, core coolant flow rate, and coolant inlet temperature.

The peaking factors for heat flux at each axial level of each fuel plate are obtained from separate detailed neutronics analysis. The Bernath CHF correlation, as is obvious from inspection of equation (1), is independent of the values of reactor heat flux. The succeeding sections describe the determination of the values of the local heat flux and the various inputs to equation (1).

3   LOCAL HEAT FLUX DISTRIBUTION

The MURR reactor core is shaped like a concentric annulus that has been formed by eight geometrically identical approximately 45° annular wedge-shaped elements. In the HEU core, each element has 24 parallel equally-spaced concentric curved fuel plates. Thus, in each element there are 23 coolant channels that have two curved fuel plates as boundaries and two end coolant channels that have only one fuel plate each as a boundary. Each end channel, which is heated by only one fuel plate, has lower bulk coolant temperatures than does its immediate neighbor, which is heated by the same fuel plate plus an additional one. Therefore, the analysis need only consider the 23 channels of each assembly that are each heated by two fuel plates. Because these 23 channels are of equal thickness, the coolant velocities are essentially the same in all 23 channels. Hence, the candidate limiting channel is selected largely by comparing nuclear power peaking factors, which characterize local and average heat fluxes and coolant channel enthalpy rise.

Identifying the most limiting channel may require assessing the margin to flow instability in several candidate channels. Of course, channels with relatively large local heat fluxes must be considered. However, channels with lesser local heat fluxes could also be limiting if their bulk coolant temperatures are relatively large and thereby lead to lower values of Bernath CHF. These would be channels where the average heat flux for each fuel plate is relatively large.

In the neutronics analysis, the heated length of the core was divided into 24 equal segments. For each fuel plate in the core, 24 values of heat flux (W/cm^2) were provided for a reactor operating power of 10 MW, one value for each of the 24 equal axial segments of the

heated length of the fuel plate. The average of these 24 values provides the average heat flux for the fuel plate. The axial heat flux distribution of each fuel plate is treated as a curve consisting of 24 uniform steps.

Table 1 provides a sample calculation which is used to demonstrate the analytical procedure for representing heat flux distribution. Columns A, B, and C of the table show the axial heat flux distribution of two consecutive plates (P01 and P02) in an element (X1). The heat fluxes shown in columns B and C were taken from the MCNP output for the week 58 HEU fuel cycle from TDR-0125[4] (the feasibility report for the conversion of the MURR core to use LEU fuel instead of HEU) with no xenon and the flux trap region only containing pool water. Since all 24 steps are of equal length, their heat fluxes can be summed and divided by 24 to obtain the average, as indicated near the bottom of the table. Obviously, plate X1P01 (column B) has the higher average and, as is obvious from the values in bold at levels 14 and 15, plate X1P01 has a higher peak heat flux than does plate X1P02. Thus, the heat flux distribution of plate X1P01 would be compared with the Bernath CHF in determining the margin to flow instability.

The axial power peaking factors for the fuel plate are obtained by dividing each of the 24 local heat flux values by the plate average heat flux value. Hence, the sum of these 24 peaking factors of the fuel plate is 24.0 and the average is 1.0. The peak of these 24 numbers is the axial peak-to-average heat flux peaking factor for the fuel plate. In Table 1, for example, the plate axial peaking factors in column D was obtained by dividing each of the corresponding 24 values in column B by the average heat flux, 129.5 W/cm^2. Column E was obtained from column C in a similar manner. The axial peak-to-average values, as shown in bold at levels 14 and 15 of columns D and E, are 1.381 and 1.378 for plates X1P01 and X1P02, respectively.

The core-average heat flux is obtained by dividing the total core power by the total core heat transfer area. The heat flux values provided by the neutronics analysis are based on the assumption that all of the reactor power, which is assumed to be 10 MW in the neutronics analysis, is deposited in the fuel plates. Since the total core heat transfer area is 17.108 m^2, the core average heat flux is 10 MW / 17.108 m^2, or 58.452 W/cm^2. The ratio of the plate average heat flux to the core average heat flux is called the "plate peaking factor". Thus, the plate peaking factor for plate X1P01 is 129.5/58.46, or 2.215. Candidate limiting channels must include those channels with the higher associated plate peaking factors.

The variation of heat flux along the azimuthal direction of each fuel plate is also taken into account. In the neutronics analysis the heated arc length along the azimuthal direction of each fuel plate is divided into a series of nine equal-radian arc length vertical strips. The average heat flux of each strip is calculated. The ratio of the highest of these nine averages to the plate-average heat flux is called the "azimuthal peaking factor". The heat fluxes provided for each level in columns B and C of Table 1 are level-averaged values rather than level azimuthal maxima.

The computer spreadsheet model does not consider the individual strips of each fuel plate. Instead, in the model, the power of each fuel plate is increased by its azimuthal peaking factor. This approach produces bounding values of local bulk coolant temperature because no credit is taken for azimuthal heat conduction in the fuel plates or azimuthal mixing in the coolant

4   ANL/RERTR/TM-11-28

channels. The hottest strip of each of the two fuel plates on either side of a coolant channel is located directly across from each other. As shown in the Table 1 sample calculations, the azimuthal peaking factors for plates X1P01 and X1P02 are 1.07 and 1.12, respectively.

In the MURR, a significant fraction, 7%, of the fission power from the fuel escapes the core as gamma or neutron radiation without creating heat in the fuel plates or in the primary coolant. Therefore, only 93% of the power contributes to the fuel plate heat fluxes and heats the primary coolant. Because all of the values of heat flux provided in columns B and C of Table 1 are based on 100% of the 10-MW core power, as is the average core heat flux of 58.452 W/cm^2, a 0.93 factor is included in the determinations of channel heat fluxes and power.

In the safety limit analysis, at each axial level of the channel, the Bernath CHF value is determined and compared with the higher of the two corresponding plate heat fluxes. In practice, this can be accomplished by using the heat fluxes of the plate with the higher product of plate and azimuthal peaking factors. Table 2 provides a sample calculation of local heat flux, including hot channel factors, which are described in Section 6. In this particular calculation, the safety limit was found to be at 14.894 MW and the limiting axial location was level 18 of the 24 axial levels. This location had the highest ratio of local heat flux to Bernath CHF based on the corresponding axial bulk coolant temperature. This heat flux ratio was 0.499999 because in the computer spreadsheet analysis the target value was set 0.499999 in order to always guarantee that the calculated maximum value would never exceed or even reach 0.5. If a different axial level were chosen for the sample calculation, the plate axial peaking factor for that other level would have been used in place of the 1.296 values shown in bold in Table 2.

4 RELATIVE DISTRIBUTION OF CHANNEL BULK COOLANT TEMPERATURE RISE

The relative distribution of bulk coolant temperature rise from the inlet to the channel to its exit is dependent on the heat flux distributions of the two fuel plates that bound the channel. In the determination of the channel bulk coolant temperature, it is assumed that the power of each fuel plate is equally divided between the two coolant channels on each side of the fuel plate. Each of the two plates that bound a coolant channel is assumed to contribute half of its power to heat the bulk coolant of the channel. This is conservative since the other channel heated by each of the two fuel plates that bound the hot channel is cooler than the hot channel and would remove slightly more than half of the heat from the common fuel plate. Thus, for each axial level the heat flux used in determining the rise in bulk coolant temperature is the average – for the two fuel plates that bound the channel – of the product of the plate axial peaking factor at the axial level, the plate peaking factor, and the azimuthal peaking factor.

For example, column F of Table 1 is a weighted average of columns D and E. For each level, half of the column D value times its plate peaking and azimuthal peaking factors (2.215 and 1.07, respectively) was added to half of the column E value times its plate peaking and azimuthal peaking factors (1.754 and 1.12, respectively) to obtain the value in column F. The sum of the values for the 24 levels in column F, 52.01, is shown at the bottom of column F. Column G is the fraction of the channel bulk coolant temperature (or enthalpy) rise that occurs

over each level and was obtained by dividing each of the 24 level values in column F by this sum. Column G sums to 1.000, or 100%.

It is worth noting that in column F of Table 1 the slight difference in fuel meat centerline arc lengths between the two fuel plates bounding the channel is ignored, thereby avoiding additional complexity. When this arc length difference is included, for the two innermost (smallest radius) plates, which are the two being considered here that bound channel 2, 48.5 % of the smaller radius plate and 51.5% of the larger radius plate would be used instead of 50.0% of each. Combining the plate peaking and azimuthal peaking factors for the two plates with a 50/50 split produces $0.500 \times 2.215 \times 1.07 + 0.500 \times 1.754 \times 1.12 = 2.1673$. Combining the plate peaking and azimuthal peaking factors for the two plates with a 48.5/51.5 split produces $0.485 \times 2.215 \times 1.07 + 0.515 \times 1.754 \times 1.12 = 2.1612$. The latter result is 0.3% smaller than the former. Thus, the difference in results is extremely small. The use of a 50/50 split is more limiting when the product of plate peaking and azimuthal peaking factors for the smaller radius plate is greater, as it is here. The effect of the difference in plate arc lengths gets smaller with increasing plate radius. For the two plates with the largest radii the weighting is 49.4/50.6.

In the analysis, the bulk coolant temperature at the exit of each of the 24 axial levels is needed. Therefore, for each axial level, the sum of all of the column G power fractions from level 1 through the level of interest must be determined. This sum of power fractions is shown in column H. For example, the value at level 5 in column H is the sum of the column G values for levels 1 through 5. When the channel bulk coolant inlet and outlet temperatures are known, then the fractions in column H can be used to obtain the channel bulk coolant temperatures at the exits of the other 23 axial levels. Thus, the temperature at each axial level is the inlet temperature plus the product of the column H value for that level and the hot channel bulk temperature rise. The determination of the increase in bulk coolant temperature between the channel inlet and the channel exit is described in the next section.

5 CHANNEL BULK COOLANT TEMPERATURES

The channel bulk coolant inlet temperature is the same as that for the core. As in the 1973 analysis of the core[2], the channel bulk coolant temperature rise is obtained from the core average value. The core average value is the core power divided by the product of core flow rate and coolant specific heat capacity at constant pressure, which in the analysis is taken to be 4.19 kJ/kg-C. Table 3 provides a sample calculation of channel bulk coolant temperature at the exit of axial level 18 for the channel bounded by plates X1P01 and X1P02. The same methodology is applicable to all other locations in the core where a channel is bounded by two fuel plates. The sample calculation includes the hot channel factors that are described in the next section.

5 HOT CHANNEL FACTORS DUE TO MANUFACTURING TOLERANCES AND OTHER UNCERTAINTIES

Manufacturing tolerances and modeling and other uncertainties can impact heat fluxes and flow rates. Past practice in MURR safety analysis[2] has been to take a bounding approach in the analysis by assuming that the most adverse extreme of each tolerance or modeling uncertainty that is considered simultaneously impacts the most limiting locations in the core.

This approach to error propagation leads to a multiplication of hot channel factors rather than a statistical combination of these factors.

Manufacturing tolerances can cause the as-built channel to be thinner than the nominal channel. A thinner channel will have a lower velocity than its nominal counterpart and its flow rate will be smaller due to both the lower velocity and smaller flow area. This is taken into account in the analysis by assuming that the limiting channel is the thinnest that is allowed by the channel thickness tolerance. For the MURR HEU core, the spacing between fuel plates is 0.080 ± 0.008 inches. Thus, the nominal channel thickness is taken to be 0.080 inches and the hot channel thickness is taken to be 0.072 inches.

Glasstone and Sesonske[5] provide a derivation for the relationship between the hot channel velocity, V_H, and the nominal channel velocity, V_N. In this derivation, they use the Blasius formula for friction factor for turbulent flow for which friction factor is inversely proportional to Reynolds number raised to the 0.25 power, i.e., $f \propto 1/Re^{0.25}$. If one uses their derivation and substitutes α for 0.25, one obtains the following relationship:

$$\frac{V_H}{V_N} = \left(\frac{D_H}{D_N}\right)^{\frac{1+\alpha}{2-\alpha}}$$

(2)

where D_H and D_N are the hydraulic diameters of the hot and nominal channels, respectively. The same relationship is also provided by Woodruff[6]. Since the ratio of the thickness to the arc length of the coolant channel is very small, the hydraulic diameter can be approximated as twice the thickness. Thus, the ratio $D_H / D_N = 0.072/0.080 = 0.90$. For $\alpha = 0.25$, the exponent in equation (2) is $1.25/1.75 = 5/7$ and the V_H/V_N, which is the hot channel factor for velocity is 0.928. In the analysis, however, a smaller values, 0.9108, is used. This was obtained by using the calculated hydraulic diameter of the narrowed limiting channel, channel 2, for D_H and the core average hydraulic diameter, which is 4 times the total core flow area divided by the total core wetted perimeter, for D_N. Hence, in the calculation D_H is 0.13876 inches, D_N is 0.15828 inches. As in Reference 5, the $5/7^{th}$ exponent is rounded off to 0.71. There, V_H/V_N is $(0.13876 / 0.15828)^{0.71} = 0.9108$.

Channel flow rate, W, is the product of channel density, velocity, and flow area. Differences in average coolant density between the hot and the nominal channels are relatively small. If these differences are ignored then:

$$\frac{W_H}{W_N} = \frac{V_H \times A_H}{V_N \times A_N} = \frac{V_H}{V_N} \times \frac{A_H}{A_N}$$

(3)

where W_H and W_N are the flow rates of the hot and nominal channels, respectively, and A_H and A_N are the flow areas of the hot and nominal channels, respectively. The area ratio, A_H/A_N is equal to the ratio of the channel thickness, or $0.072/0.080 = 0.90$. Since V_H/V_N is 0.9108, W_H/W_N, which is the hot channel factor for flow, is $0.9108 \times 0.90 = 0.8197$.

The average density of U^{235} in the fuel matrix of the plate has a tolerance that affects plate power and heat flux. The power produced by the plate is proportional to its U^{235} density. If both plates that bound a channel are at their upper limits of U^{235} density in the fuel matrix, then the channel power increase due to this effect will be at its maximum. For example, if both plates have average fuel densities that are 3% above their nominal values, as is assumed in the current analysis, then the channel power, bulk coolant temperature rise, and average heat flux will be 3% higher. The assumption that both plates are at the upper limits of this tolerance is a bounding one.

Another manufacturing tolerance that applies to power is the fuel meat thickness. Sometimes there can be relatively large local variations in thickness in a fuel meat whose average thickness is close to its nominal value. The local variations in thickness directly impact the local heat flux, but have little impact on the bulk coolant temperature. Therefore, two hot channel factors can be used to represent the variations in fuel meat thickness – a relatively large factor, such as 1.15, which is applied to the local heat flux calculation, and a relatively small hot channel factor, such as 1.03, which would be applied to bulk coolant temperature rise. These are the values that are used in the current analysis and are consistent with Vaughan[2].

The sample calculations in Tables 2 and 3 include an "additional allowable peaking factor" of 1.062 in the overall power peaking factors for heat flux and enthalpy rise. This calculates the total overall peaking factor with which a MURR core can safely operate.

6 CHANNEL BULK COOLANT VELOCITY

The velocity at the inlet to the limiting channel is calculated as V_H of equation (2) in section 6, where V_N is the average inlet velocity for the entire reactor core and D_H, D_N, and the exponent $(1+\alpha)/(2-\alpha)$ are 0.13876, 0.15828, and 0.71, respectively, as explained in section 6. The channel velocity gradually increases from the inlet to the outlet of the channel due to the small reduction in coolant density with increasing coolant temperature. Flow rate is the product of local coolant density, flow area, and local coolant velocity. Since the flow area is assumed uniform over the entire channel length, local velocity is inversely proportional to local coolant density. Table 4 provides a sample calculation of local coolant velocity in a limiting channel at level 18.

7 CHANNEL EXIT COOLANT PRESSURE

For the analysis the pressure between the fuel plates at the exit of the limiting fueled channel is needed. The MURR technical specifications specify the minimum allowed pressure at the reactor pressurizer. Thus, a model is needed to determine the pressure drop from the pressurizer to the exit of the limiting channel. This pressure drop depends on flow rate and coolant temperature. Coolant temperatures in the core are a function of core inlet temperature, flow rate, and power.

The model provided by Reference 2 for the pressure drop from the pressurizer to the core exit was investigated by J. C. McKibben of MURR. Through measurements and analysis during March through May of 2011 he made substantial improvements to the determination of this

pressure drop. Since a formal document describing his work is not available at this time, an overview, based on discussions with him, will be presented here and will be contrasted with the Reference 2 model, which has been used for MURR safety analysis in the past.

In the Reference 2 model the path from the pressurizer to the core exit is divided into 13 parts. Each part is called a component. Each component has a single flow path or consists of two identical parallel paths. Each component has the same total flow rate. The coolant temperature through the first 12 components, which lead up to the core inlet, is the inlet temperature. The 13th component is the reactor core. Its coolant temperature is taken to be the mean of the core inlet and mixed-mean coolant outlet temperatures. The required pressure drop to the core outlet is the sum of the 13 component pressure drops.

For a known coolant temperature, T_0, of 155° F at the reactor inlet (or 165° F average through the core) and a known reactor flow rate, Q_0, of 3600 gpm, assumed known component pressure drops, ΔP_0, are provided, as shown in Table 5. As the table indicates, one combined value of ΔP_0 is provided for the pressure drop across components 1, 2, and 3 taken together and another is provide for components 5 through 10. For components 1 through 4, Q_0 is shown in the table as 1800 gpm. However, as indicated in the table, for each of these components, this value is for each of two parallel paths. Thus, in the table the total flow rate, or effective Q_0, through each component is 3600 gpm. Reference 2 provides two scaling relationships that enable pressure drops, ΔP's, to be determined for other values of flow rate, Q, and coolant temperature, T. These two relationships are:

$$\frac{\Delta P}{\Delta P_0} = \left[\frac{\rho(T)}{\rho(T_0)}\right]^{1.0} \left[\frac{Q}{Q_0}\right]^{2.0} \tag{4}$$

$$\frac{\Delta P}{\Delta P_0} = \left[\frac{\rho(T)}{\rho(T_0)}\right]^{0.8} \left[\frac{Q}{Q_0}\right]^{1.8} \left[\frac{\mu(T)}{\mu(T_0)}\right]^{0.2} \tag{5}$$

where ρ is coolant density, μ is coolant dynamic viscosity. Equation (4) is for the portions of the flow path that are characterized by non-frictional losses, such as changes in flow area and/or flow direction, as opposed to being due to wall friction in a duct. Equation (5) is for portions of the path that are characterized by wall friction (frictional) losses. Components 4 and 12 are shown in Table 5 to be non-frictional. The rest, as indicated in Table 5, are frictional.

Both equation (4) and equation (5) can be derived from well-known hydraulic relationships for turbulent flow. In the derivation of equation (5) it is assumed that the friction factor is proportional to the Reynolds number raised to the −0.2 power.

For pair values of core flow rate, Q, and inlet temperature, T, equation (4) can be evaluated once for the two non-frictional components, 4 and 12, and equation (5) can be evaluated once for the all of the other components in Table 5, except for the core. For example, for a flow rate of 3200 gpm and an inlet temperature of 155° F, $\Delta P/\Delta P_0$ from equations (4) and (5) are 0.7901 and 0.8090, respectively. The corresponding pressure drop from the pressurizer to the core inlet is: 0.7901 × [0.2689 + 0.8980] psi + 0.8090 × [3.259 + 4.08 + 0.1977] psi =

0.7901 × [1.1669] psi + 0.8090 × [7.5367] psi = 7.02 psi. The value of T for the core depends on the core temperature rise, which is a function of core power, which is initially unknown.

Figure 1, which is the basis for the new model, shows a schematic representation of the piping that carries coolant flow to the reactor core. In the figure the total core flow rate is 3600 gpm. 1825 gpm enters from the left through Loop A and another 1825 gpm enters through Loop B. At point 2 50 gpm is extract from the Loop A flow and goes to the deionizer. At point 3 the remaining 1775 gpm of the Loop A flow merges with the 1825 gpm of the Loop B flow to form the combined flow of 3600 gpm that goes through the core.

The deionizer flow remains constant regardless of core flow. Thus, for a 3200 gpm core flow rate, which is the minimum allowed by the Limiting Safety System Settings (LSSS) conditions as defined by the Technical Specifications for the MURR HEU core, the 1825 gpm values in Figure 1 would be replace by 1625 gpm, 50 gpm would go to the deionizer, as before, 1575 gpm would flow from point 2 to point 3, and the core-flow would be 1575 gpm + 1625 gpm, which is 3200 gpm.

For the new model J. C. McKibben used hydraulic handbook data to predict the irrecoverable pressure drops between point 1 and 5 of Figure 1. He also employed measured data taken on March 27, 2011 on the MURR plant with the eight core fuel elements in the reactor vessel with the reactor operating at 10 MW. Also, measurements were taken on March 28, 2011 with the eight core fuel elements out of the reactor vessel, but with the primary coolant system operating. The locations where pressure measurements were made are indicated in Figure 1 by the letter "P" inside a circle. The pressure difference, which is indicated in Figure 1 by "ΔP" inside a circle, was also measured. Coolant flow rate and temperatures were also measured.

J. C. McKibben used the two sets of measurements to calibrate and adjust his analytical/handbook predictions of irrecoverable pressure drop and better determine the pressure drop across the core. Then he used his benchmarked hydraulics model to produced Table 6, which is the new model equivalent of Table 5 in the Reference 2 model. In Table 6 the core reference flow rate is 3608.3 gpm instead of 3600 gpm. This is because J. C. McKibben intended that in the application of equation (5) to the core, each volumetric flow rate be evaluated at its core average density, which is taken to be the density corresponding to the average of the core inlet and outlet temperatures. Thus, for a reference inlet flow rate of 3600 gpm, the Q_0 is the 3600 gpm × ρ_{inlet} / $\rho_{average}$, where ρ_{inlet} and $\rho_{average}$ are the inlet and average density of the coolant, respectively. Hence, the reference flow rate for the core, Q_0, is 3608.3 gpm instead of 3600 gpm. Similarly, if the actual core inlet flow rate is 3200 gpm, then Q for the core in equation (5) is 3200 gpm increase by a factor of the ratio of inlet and average core coolant densities.

Since there was no measurement at point 5 of Figure 1, J. C. McKibben deliberately overestimated the pressure drop up to point 5 so that the pressure predicted at point 5 would tend to be lower and more limiting than it would otherwise be. Thus, his approach was to deliberately err on the safe side where there is uncertainty. In the new model equations (4) and (5) are used in the same manner that they are used in the Reference 2 model, except that in the new model Q for the core corresponds to the core average density rather than the inlet density.

The nitrogen gas pressure inside the pressurizer is the measured pressurizer pressure used in the operation of the reactor. A 2-inch diameter pipe connects the bottom of the pressurizer to the 8-inch diameter Loop A pipe at point 1. Point 1 is 608 feet and 6 inches above sea level. The nominal level of the water in the pressurizer is 48 inches below point 1. The primary charging pump starts adding water to the pressurizer when the level gets down to 6 inches below the nominal value. If the pressurizer level falls so that it is 16 inches below its nominal value, a scram is initiated. The beginning of the reactor fuel plates at the core inlet is 15.25 inches below point 1. The exit of the core fuel plates, which is taken to be the core exit, is 25.5 inches below the core fuel plate inlet. These dimensions are important in the new model because it includes pressure differences due to gravity heads. The temperature in the pressurizer and in the 2-inch diameter pipe between the pressurizer and point 1 is taken to be 85° F in the analysis. For the analysis, the most limiting pressurizer level allowed was used. This level is the scram level, which is 64 inches below point 1. For the reactor at the LSSS limiting condition of flow rate, pressure, and inlet temperature (3200 gpm, 75 psia at the pressurizer, and 155° F) and a core power of 14.894 MW, which is the core power at which the new model predicts flow instability to occur, the inclusion of the gravity heads in the model causes a 0.867 psi reduction in core exit pressure. This effect was not included in the Reference 2 model.

For a core flow of 3200 gpm, the flow velocity in Loop A in the 8-inch pipe at point 1 is 10.4 ft/s and the core average velocity between the fuel plates at the core exit, point 5 in Figure 1, is 21.1 ft/s. The new model uses Bernoulli's equation to determine the decrease in pressure caused by increasing the fluid velocity from 10.4 ft/s second to 21.1 ft/s. This effect is included in the new model, but not in the Reference 2 model. For the reactor at the LSSS limiting condition of flow rate, pressure, and inlet temperature and a core power of 14.894 MW, this effect causes a 2.18 psi reduction in pressure at the core exit.

For the reactor at the LSSS limiting condition of flow rate, pressure, and inlet temperature and a core power of 14.894 MW, the irrecoverable pressure drop[†] from point 1 of Figure 1 to the point 4 is 7.02 psi in the Reference 2 model and 7.87 psi in the new model and the core (frictional) pressure drop is 9.90 psi in the Reference 2 model and 10.39 in the new model. These four pressure drop values are obtained by using equations (4) and (5) to scale the pressure drops of Table 5 or 6. Thus, the irrecoverable pressure drop from point 1 to the core exit, point 5, is 7.87 + 10.39, or 18.26 psi, in the new model, which is to be compared to 7.02 + 9.90, or 16.92 psi, in the Reference 2 model. Hence, the irrecoverable pressure drop from point 1 to point 5 is 1.34 psi greater in the new model. When this greater pressure drop is combined with the two pressure drops not included in the Reference 2 model, which are the 0.87 psi pressure drop due to gravity heads and the 2.18 psi pressure drop due to velocity increase, the new model predicts a core exit pressure of 75 − 18.26 − 0.87 − 2.18, or 53.7 psia, which is 4.4 psi lower than the 75 − 16.92, or 58.1 psia, of the Reference 2 model. If the pressure at the core exit were to be increased by 4.4 psi to 58.1 psia, the allowed reactor power for the LSSS limiting condition of flow rate, pressure, and inlet temperature would be increased by 0.51 MW to 15.4 MW.

[†] Irrecoverable pressure drops include the non-frictional pressures drops that employ the scaling equation (4) and the frictional pressure drops that employ the scaling equation (5). They do not include the recoverable pressure changes due to changes in elevation or velocity.

8 AN ALTERNATIVE APPROACH TO CORE PRESSURE DROP DETERMINATION

The Bernoulli equation is $P_1 + \rho V_1^2 / 2 + \rho g Z_1 = P_2 + \rho V_2^2 / 2 + \rho g Z_2$, where P is pressure, ρ is density, V is velocity, g is acceleration due to gravity, Z is elevation and is increasing in the upward direction, and the two subscripts 1 and 2 refer to two different locations in the fluid, where 2 is downstream of 1. This equation can be modified to include the irrecoverable pressure drop between points 1 and 2 by adding a term to the right side of the equation, such as $(K + f L/D) \rho V^2 / 2$, where K is a form loss, f is the Moody friction factor, L is path length, D is path hydraulic diameter, V, is a velocity associated with K and f. In both the Bernoulli and the modified Bernoulli equations the density ρ is a constant. When differences in density are small, such as in the reactor core, some analysts still use the modified Bernoulli equation and get around the constant-density limitation by using an average density between points 1 and 2 when evaluating irrecoverable losses due to friction and when evaluating differences in pressure due to changes in elevation. This is a reasonable approach and is used in the new model.

An alternative approach for the MURR application is to apply the modified Bernoulli equation between the points 1 and 4 of Figure 1, where density is constant, and apply the integral form of the momentum equation from points 4 to 5. In this case, points 4 and 5 are located between the two fuel plates that form the limiting, or hot, channel, which is channel 2 in the analysis. These fuel plates are the two of the smallest arc length and closest to the flux trap in MURR element 1.

The limiting channel between inlet level a and outlet level b (or points 4 and 5 in Figure 1) is modeled with the integral form of the momentum equation. The control volume used in the model is the volume contained inside the wetted perimeter of the channel between levels a and b. For a steady-state process the general form of this equation is:

$$\vec{F}_s + \int_{C.V.} \vec{B} \, d\upsilon = \int_{C.S.} \vec{V} \rho \left(\vec{V} \bullet d\vec{A} \right) \tag{6}$$

where, the first integral is an integral over the control volume, C.V. and the second integral is an integral over the control surface, C.S. This vector force-balance equation, which can be obtained from a fluid dynamics textbook,[7] is applied here only in the vertical, or z, direction. The positive direction is chosen to be downward and in the direction of flow from point a to point b. The first term, $\vec{F}_s$, represents the sum of the forces on the control volume surface, such as those due to pressure and shear stress. The second term is an integral of all of the body forces, $\vec{B}$, such as those due to gravity, acting within the control volume. The third term is the momentum flux term and is integrated over the control surface. This term arises because equation (6) is focused on a fixed volume in space in which mass enters and leaves, rather than on a fixed mass. The z-component of the above vector equation yields:

$$A_c \left(P_a - P_b \right) - p_{wetted} \int_a^b \tau(z) \, dz + g A_c \int_a^b \rho(z) \, dz = \frac{W_c^2}{A_c} \left(\frac{1}{\rho_b} - \frac{1}{\rho_a} \right) \tag{7}$$

where P_a and P_b are the pressure at the inlet and the outlet of channel, respectively, p_{wetted} is the wetted perimeter of the channel, $\rho(z)$ is the coolant density of the channel, which varies along the length of the channel, $\tau(z)$ is the shear stress along the perimeter of the channel, which also varies along the length of the channel, ρ_b is the coolant density at the exit of the channel, and ρ_a is the coolant density at the inlet to the channel. Both integrals in equation (7) are always positive. The negative sign ahead of the shear force term is needed because the shear forces are always in the direction opposite of the flow direction, which is the positive direction.

The first term of equation (7) is due to the pressure difference between the inlet and the outlet of the channel. The second term is due to the friction, or shear force, at the channel surfaces. These first two terms correspond to the first term of equation (6). The third term of equation (7), which is due to gravity, corresponds to the second term of equation (6). The last term of equation (7) corresponds to the last term of equation (6). This term is equal to the channel flow rate, W_c, times the exit velocity at b minus the inlet velocity at a.

The shear stress is related to the Darcy (Moody) friction factor, f, by the following relationship:

$$\tau(z) = \frac{f(z)}{8} \frac{W_c^2}{\rho(z) A_c^2} \tag{8}$$

The wetted perimeter and the flow area are related by the definition of hydraulic diameter. Hence:

$$p_{wetted} \equiv \frac{4 A_c}{D_h} \tag{9}$$

where D_h is the hydraulic diameter of the channel.

Equations (7), (8), and (9) can be combined to yield:

$$P_b = P_a - \frac{W_c^2}{2 D_h A_c^2} \int_a^b \frac{f(z)}{\rho(z)} dz + g \int_a^b \rho(z) dz - \frac{W_c^2}{A_c^2} \left(\frac{1}{\rho_b} - \frac{1}{\rho_a} \right) \tag{10}$$

The last three terms on the right side of equation (10) are the friction pressure drop, the gravity term, and the momentum flux term, respectively. In equation (10) W_c/A_c is the channel mass flux, G_c, which is constant along the length of the channel and is the product of the local density and local velocity. The integrals in the friction pressure drop and gravity terms can be estimated by numerical means that divide the length from a to b into smaller regions. A simpler, and reasonably accurate, approach for the MURR application is to assume that all of the fluid in the region between a and b is at a constant temperature that is the mean of the hot channel coolant inlet and the outlet temperatures.

The new model (developed by J. C. McKibben) has analogous friction pressure drop and gravity terms to those in equation (10) that are based on the average core channel rather than the hot channel. The new model uses the mean of the core inlet and outlet temperatures in

evaluating the corresponding two integrals in its model. It does not have a momentum flux term, which, as shown below, is extremely small.

In order to demonstrate that the new model produces a pressure for use with the Bernath equation, equation (1), that is at least as low as that produced by equation (10), the pressure drops over the core region that is produced by each of the two approaches will be compared for the LSSS values of flow, inlet temperature, and pressurizer pressure (3200 gpm, 155° F, and 75 psia) and a reactor power of 14.894 MW. The hot channel inlet velocity and hydraulic diameter are used in evaluating equation (10). The hot channel inlet velocity of 18.99 ft/s is the product of the core average velocity (3200 gpm divided by the 0.3419 ft^2 core flow area), 20.85 ft/s, and the hot channel factor on velocity, 0.9108. As explained in section 6 with reference to equation (2), the hot channel hydraulic diameter is 0.13876 inches.

In the new model the application of the modified Bernoulli equation to the MURR, assumes that location 1 is at point 1 in Figure 1 and location 2 is between the fuel plates and at point 5 of Figure 1. In the new model ρ and V_2 are the core-averaged exit values. The equation (10) hot channel approach assumes that in the modified Bernoulli equation location 1 is also at point 1 in Figure 1, but location 2 is between the fuel plates and at the hot channel inlet. Table 7 compares the Bernoulli velocity pressure drop term, $\rho V_2^2 / 2$, and the friction, gravity, and momentum flux, pressure drops from point 4 to point 5 of Figure 1 for the new model with those associated with the use of equation (10) to model the pressure drop across the hot channel for LSSS values of flow, inlet temperature, and pressurizer pressure (3200 gpm, 155° F, and 75 psia) and a reactor power of 14.894 MW. The hot channel modeling causes $\rho V_2^2 / 2$ to be 2.378 psi, which is lower than the new model value, 2.897 psi, by a factor of the product of the square of the hot channel factor on velocity and the ratio of the core outlet to inlet densities, or $0.9108^2 \times 968.2 / 978.4$, or 0.821.

In Table 7 the new model core friction pressure drop, 10.394 psi, is the product of 13.8049 psi, which is the component 8 reference pressure drop of Table 6, and 0.7529, which is the scale factor provided by equation (5) to correlate a the pressure drop at reference conditions of core flow of 3608.3 gpm at a core average reference temperature of 128.68° F to the pressure drop at core conditions of 3200 gpm based on the inlet temperature and the core average temperature is 170.06° F. Before equation (5) can be evaluate, the 3200 gpm flow rate must be increased by a factor of the ratio of the inlet and outlet densities, 978.4/973.5, or 1.0050, so that it corresponds the volumetric flow at the average core density. Hence, 3200 gpm × 1.0050, or 3216 gpm, is the value of Q used in equation (5).

The equation (10) friction pressure drop used the mean of the inlet and outlet temperatures of the hot channel, 68.33° C (155° F) and 118.2° C (244.8° F), respectively. This mean temperature is 93.28° C (199.90° F). The viscosity was evaluated at this temperature and, along with the hot channel mass flux and the hydraulic diameter, produced a Reynolds number of 65681. The mass flux, or flow rate divided by the flow area, G_c, 5664 kg/m^2-s, was obtained as the product of the hot channel inlet velocity and inlet density.

The hot channel relative roughness is needed to obtain the hot channel friction factor. Based on the 1989 MURR Drawing 13005, Rev. 6, Note 5, the maximum absolute roughness of

the MURR HEU fuel plate is 63 micro inches. The relative roughness, 0.0004540, is the ratio of the absolute roughness to the hydraulic diameter. This relative roughness and the 65681 Reynolds number were used in the Colebrook equation, which is the basis for the turbulent portion of the Moody diagram, to obtain a friction factor of 0.02143.

The Colebrook equation is:

$$\frac{1}{\sqrt{f}} = 2\log_{10}\left(\frac{\varepsilon/D}{3.7} + \frac{2.51}{Re\sqrt{f}}\right)$$ (11)

where f is the friction factor, ε/D is the relative roughness, and Re is the Reynolds number. A solver built into the Excel computer spreadsheet program was used to evaluate the above transcendental equation for f. With the approximation of constant density and friction factor, the friction pressure drop integral of equation (10) becomes f L/D $G_c^2/(2\ \rho)$, where L is hot channel length, 25.5 inches. The hot channel friction pressure drop was found to be 9.515 psi.

As an interesting aside, the above friction pressure drop analysis for the hot channel that employed equation (11) was repeated to predict the core pressure drop at the Table 6 reference conditions of core average temperature of 128.68° F and the volumetric flow rate for this temperature of 3608.3 gpm. This temperature and flow rate, and the core hydraulic diameter, as provided above in section 6, of 0.15828 inches were used in the calculation. Since the average core pressure is close to 4 bar, the NIST steam tables were used to determine the density and the viscosity of the coolant at this pressure and 128.68° F. The Reynolds number was found to 55276. A core pressure drop, f L/D $G_c^2/(2\ \rho)$, of 12.937 psi was obtained. Equation (5) can be used to scale this pressure drop to correspond to the Table 7 conditions of 3200 gpm at 170.06° F. The equation (5) scaling factor is 0.7529 and the resultant core pressure drop is 9.740 psi. This value is very close to the hot channel pressure drop of 9.515 psi for the same Table 7 reactor conditions. This is to be expected because both pressure drops were calculated by the same method that employed the friction factor provide by equation (11) and because both the hot channel and all other core channels share common inlet and outlet plena.

The Table 6 value of core pressure drop was deduced by J. C. McKibben based on analysis of measured data taken on the MURR plant with the core in place and with the core removed. He deliberately chose a core pressure drop on the high side of the tolerance band that resulted from uncertainty in measurement and calculation. The 12.937 psi value calculated above with the aid of equation (11) is based on the common practice for turbulent flow of using the friction factor for a round duct of the same hydraulic diameter as the one being investigated. The ratio of the measure to the calculated core pressure drops is 13.8049/12.937, or 1.067. However, reference 8 provides that turbulent flow friction factors in smooth-walled rectangular ducts within ±5% of experimentally measure values can be obtained as the product of the friction factor for circular duct and the factor (1.0875 − 0.1125 × α*), where α* is the aspect ratio of the rectangular duct. The MURR coolant channels can be approximated as rectangular ducts with aspect ratios between about 0.02 and 0.04, causing (1.0875 − 0.1125 × α*) to be between 1.085 and 1.083, respectively. When 1.083 is combined with the 12.937 psi core pressure drop calculated above, the result, 14.01 psi, is only 1.5 % greater than the 13.8049 psi deduced by J. C. McKibben and listed in Table 6. Hence, 13.8049 psi is a very reasonable value.

The gravity head term is calculated the same way in the hot channel approach as in the new model except that in the hot channel approach the density is evaluated at the mean of the hot channel inlet and outlet temperatures rather than at the mean of the core inlet and outlet temperatures. Both approaches use the same core length of 25.5 inches. The gravity head is the product of density, acceleration due to gravity, and length. The new model predicts a gravity head pressure increase of 973.5 kg/m^3 × 9.80665 m/s^2 × (25.5 in × 0.0254 m/in) / (6894.757 Pa / psi), or 0.897 psi and the hot channel approach yields 962.7 kg/m^3 × 9.80665 m/s^2 × (25.5 in × 0.0254 m/in) / (6894.757 Pa / psi), or 0.887 psi.

The momentum flux term of equation (10) is evaluated as the product of the square of the hot channel mass flux and the difference of the reciprocal of the hot channel exit density and the reciprocal of hot channel inlet density, (5664 kg/m^2/s)^2 × (1/(943.5 kg/m^3) − 1/(978.4 kg/m^3)) = 1213 Pa = 0.176 psi. This very small term, which reduces the exit pressure, is not present in the new model.

The totals at the bottom of Table 7 show that for the representative limiting test case that the pressure at point 5 of Figure 1 will be 1.2 psi lower for the new model than when the equation (10) approach is used to predict the overall pressure drop for the hot channel. Since a lower exit pressure produces a lower allowed core power, the new method tends to err on the safe side.

9   HYDRAULIC DIAMETER (D$_E$) AND HEATED DIAMETER (D$_I$)

The channel hydraulic diameter (D$_e$), which is four times the flow area divided by the wetted perimeter, and the channel heated diameter (D$_i$), defined as the heated perimeter divided by π, can easily be determined for each channel in the MURR core. Since in the analysis the limiting channel flow rate and velocity are based on the hot channel thickness of 0.072 inches rather the nominal channel thickness of 0.080 inches, the value of D$_e$ for use in equation (1) is also based on the hot channel thickness. Similarly, D$_i$ is based on the minimum arc lengths allowed by the manufacturing tolerances.

The two fuel plates represented in Table 1 are the innermost two fuel plates and bound the second channel, where the first channel is the one adjacent to the cylindrical inner vessel wall. For the corresponding hot channel, channel 2, the value of hot channel D$_e$ is 0.13876 inches, or 0.011563 feet, and D$_i$ is 1.0784 inches, or 0.089867 feet.

10 COMPUTER SPREADSHEET IMPLEMENTATION

Table 8, which spans five pages, shows the computer spreadsheet that was used to predict the allowed reactor power for the LSSS combination of reactor inlet temperature of 155° F, pressure at the pressurizer of 75 psia, and total core flow rate of 3200 gpm. This table also includes the heat flux peaking factors and the hot channel factors described above. This example is also consistent with the sample calculations provided in Tables 1 through 4.

The rows of Table 8 are numbered 1 through 100. The columns are identified by letters A through O. The inputs to the spreadsheet have a color shading of yellow. These can be found

on pages 2 through 5 of the table and are describe further below. The cell with allowed reactor power output, cell B53, can be found page 2 and has a color shading of light turquoise.

The spreadsheet has two steps. Step 1 starts near the top of Table 8 on line 2. Step 2 starts on line 59 at the top on page 3. In step 1 the pressure at the reactor outlet (cell B51) is determined for use in step 2. In step 2 on line 95 the ratio of channel heat flux to Bernath CHF is determined for each level from levels 12 through 24 of the channel. This ratio is not calculated for levels 1 through 11 because the limiting location cannot occur before level 12. This is because the peak heat flux does not occur before level 12 and the coolant temperature is rising monotonically from the inlet to the outlet. The ratios at levels 12 through 24 are compared and the largest ratio is repeated in cell O95. Cell O96, which has light turquoise shading, provides the level at which the maximum occurred. As explained above, the maximum desired heat flux ratio (cell B71) is 0.499999 instead of 0.5. The value in cell B96 is the desired maximum value (cell B71) minus the maximum heat flux ratio (cell O95). Adjusting the power in cell B53 until the value in cell B96 is zero would provide a maximum heat flux ratio of 0.499999. Cell B98, which has a light turquoise shading, is the degrees Celsius of subcooling at the hot channel exit. This value, which is the saturation temperature (cell B75) minus the hot channel exit temperature (cell B74), must not be allowed to become negative. Cell B100 is the minimum of cell B96 and B98. In concept, the reactor power in cell B53 would be gradually increased from a low value until either the subcooling at the channel exit, cell B98 reaches zero or cell B96 equal zero, which implies that the maximum heat flux ratio is 0.499999. A solver in the spreadsheet is used to automatically do this adjustment and determine the maximum allowed reactor power in cell B53. Since step 1 also uses the value of reactor power in cell B53 to determine the pressure at the exit of the core, the reactor exit pressure obtained in step 1 is consistent with the reactor power level that is obtained in step 2.

There are five contiguous sets of boxes on page 1 of Table 8 that have a colored rectangular boundary. The values in the light-blue bounded box, cell B4 through cell F13, were taken from Table 6 and are used in conjunction with equations (4) and (5) to obtain the pressure drop from the pressurizer to the core exit. The five pressures in the first set of green bounded box, lines 15 through 19, are the sum of the frictional and non-frictional pressures at 120° F. The five P/P$_0$ values in the second green bounded box, lines 21 through 25, correspond to the first set of green bounded boxes. Thus, the frictional pressure drop for the 1825 gpm leg of the Figure 1 flow schematic (from point 1 to point 2) is the product of cells B15 and B21. Similarly, cells B16 and B22 correspond to frictional pressure drop from point 3 to point 4, cells B17 and B23 correspond to non-frictional pressures drop from point 1 to point 2, cells B18 and B24 correspond to the non-frictional pressure drop from point 2 to point 3, and B19 and B25 correspond to the non-frictional pressure drop from point 3 to point 4. The sum of the products of these five pairs is the irrecoverable pressure drop from the pressurizer to the core inlet (point 1 to point 4), 7.875 psi in cell B47.

The values in the medium-blue bounded box are polynomial curve fits to steam table value of density and viscosity at 5 bar for temperatures between 40 and 100° C in increments of 1° C. These functions are of the form $y = a0 + a1 \times T + a2 \times T^2 + a3 \times T^3$, where y is density in kg/m^3 or viscosity in micro Pa s and T is temperature in °C. The values in the brown-bounded boxes use the curve fits in the medium-blue bounded box to obtain values of density and

viscosity for six temperatures. The first two temperatures in the brown-bounded boxes are the two reference temperatures in the light-blue bounded boxes, the next three are the core inlet, average of inlet and outlet, and outlet temperatures, and the last temperature is that of the pressurizer pipe and water.

The input values in cells B54 through B56 are self evident. The input value in cell B61 is the fraction of reactor power that contributes to the fuel plate heat fluxes and primary coolant temperature rise, 0.93. The input values in cells B62, B65, and B68 are hot channel factors, which are provided in section 6, above.

The power factor for enthalpy rise without additional factor, cell B63, 2.299, is Item C of Table 3. It is the product of a 1.03 hot channel factor on fuel content (maximum overload for a plate), a 1.03 hot channel factor on fuel meat thickness (tolerance factor on average fuel meat thickness) and a 2.167 factor that results from combining plate average and azimuthal peaking factors for plates X1P01 and X1P02 of Table 1. The 2.167 factor is calculated in the middle of Table 3. The product of 1.03, 1.03 and 2.167 is 2.299 (cell B63).

Cell B66, the power factor for heat flux without axial factor or additional factor, is Item C of Table 2. It is the product of a 1.03 hot channel factor on fuel content, a 1.15 hot channel factor on (local) fuel meat thickness, a 2.215 plate average peaking factor, and 1.07 plate azimuthal peaking factor, which is 2.807.

The heat transfer area needed for cell B69 is the product of the nominal fuel meat length (24 inches) and twice the sum of the nominal arc lengths of the fuel meats of all of the fuel plates in the core. This was found to be 184.15 ft^2. The flow area in cell B70 is the sum of the nominal flow areas of all 200 channels in the entire core, 0.3419 ft^2. These values are to be compared with those in Reference 2, 184.28 ft^2 for core heat transfer area and 0.3505 ft^2 for the core flow area. The input value for levels 12 through 24 that are needed for lines 78 and 79 can be found in columns D and H, respectively, of Table 1. The input D_e and D_i value in cells D86 and D87, respectively, can be found in section 10, above.

The "overall power factor for heat flux" on line 80 is the product of 2.9814 in cell B67, which is labeled "power factor for heat flux without axial factor & with add'l factor", and the plate axial peaking factor, which is on line 78. The saturation temperature at the core exit in cell B75 is based on a polynomial curve fit to steam table values over a range of pressures from 30 to 85 psia in steps of 5 psi. Lines 80 through 93 are used to evaluate the Bernath CHF. The values on line 92 are 1.8 times those on line 91. The values on line 93 are 3.152481×10^{-6} times those on line 92.

11 DISCUSSION – MOTIVIATION FOR CURRENT ANALYTICAL MODEL DEVELOPMENT

The preceding sections have described the implementation of a methodology in considerable detail. The motivation for undertaking this effort at this time is that an error was found in the manner in which D_i is defined in Reference 2. In the Bernath paper,[1] D_i is defined in the nomenclature section to be "diameter of heated surface (heated perimeter divided by π), ft.

(in.)". In the paper D_i is referred to as the "heated diameter", as can be see in the caption of Figure 1 of the paper. Other authors define "heat diameter", D_{heated}, to be 4 times the flow area divided by the *heated* perimeter. This definition is analogous to hydraulic diameter, D_e, which is defined as 4 times the flow area divided by the *wetted* perimeter. For a test section consisting of liquid flowing inside a round heated-wall tube, the two definitions of heated diameter lead to the same value. However, when the flow cross section is a thin annulus formed by a round heating element inside a round enclosure or in the case of a thin rectangular duct heated along the two longer sides, the second (D_{heated}) definition can produce a value of heated diameter that is an order of magnitude smaller than the one in the Bernath paper.

While comparing his correlation to experimental data, Bernath[1] provided values of D_i and D_e for specific experiments. One of these experiments, the W.A.P.D. data,[9] is for flow in a thin rectangular duct. The abstract of Reference 9, which is available online from OSTI, indicates that the duct dimensions are 0.097 inches by 1 inch by 27 inches long. Thus, $D_e = 4 \times (0.097 \times 1)/(2 \times (0.097 + 1))$ inches = 0.177 inches. If we assume that the two 1-inch sides of the rectangular duct are heated and the two 0.097-inch ones are not heated, then $D_i = 2 \times 1 / \pi$ inches = 0.637 inches. These values of D_e and D_i are the ones cited by Bernath. Using 4 times the flow area divided by the heat perimeter (D_{heated}) for D_i would produce 0.194 inches for a 2-inch heated perimeter. Thus, this example shows that for rectangular ducts Bernath intended that D_i be the heated perimeter divided by π.

In both References 2 and 3, D_i is referred to as the "heated hydraulic diameter". On page 14 of Reference 2 the "heated-to-wetted perimeter ratio" is given as 0.924. This ratio, which is D_e / D_{heated}, was used in the Reference 2 safety analysis of the MURR reactor to incorrectly obtain D_i. Separate calculations of the heated and wetted perimeters of all MURR channels that are heated by two fuel plates show that this ratio ranges from about 0.88 for the first channel heated by two fuel plates (smallest radius) to 0.94 for the last. The Reference 2 analysis was closely replicated in Appendix B-1, "Replication of MURR 1974 10 MW Upgrade Safety Analysis," of TDR-0125[4] (the feasibility report for the conversion of the MURR core to use LEU fuel instead of HEU). In the replication D_i was taken to be $D_e/0.924$. D_e was taken to be 0.15573, as provided in Reference 2. Thus, Appendix B-1 of Reference 3 repeated the error in D_i in its replication of the Reference 2 results.

12 CONCLUSION

The model that was used to perform flow instability analysis for the MURR HEU core has been described in sufficient detail to enable one to independently reproduce the results of the analysis. Table 8 shows the computer spreadsheet model that was used to implement the model. Tables 1 through 4 provide sample calculations of key input parameters that are used in the Table 8 model. Key aspects of the new model developed by J. C. McKibben to determine the pressure drop from the pressurizer to the core exit are explored and explained.

REFERENCES

1. Louis Bernath, "A Theory of Local-Boiling Burnout and Its Application to Existing Data," *Chemical Engineering Progress Symposium*, Series No. 30, Volume 56, pp. 95-116 (1960).

2. F. R. Vaughan, *Safety Limit Analysis for the MURR Facility*, NUS-TM-EC-9, prepared for the University of Missouri by the NUS Corporation, 4 Research Place, Rockville, Maryland, 20850, May 1973.

3. University of Missouri Research Reactor Safety Analysis Report, Chapter 4, Reactor Description, submitted to the U.S. Nuclear Regulatory Commission in 2006.

4. Feasibility Analysis for HEU to LEU Fuel Conversion of the University of Missouri Research Reactor (MURR), TDR-0125, University of Missouri-Columbia Research Reactor, Columbia Missouri, September 30, 2009.

5. Samuel Glasstone and Alexander Sesonske, *Nuclear Reactor Engineering*, Third Edition, Van Nostrand Reinhold Company, New York, 1981, pp.407-408.

6. W. L. Woodruff, *Evaluation and Selection of Hot Channel (Peaking) Factors for Research Reactor Applications*, ANL/RERTR/TM-28, RERTR Program, Argonne National Laboratory, Argonne, Illinois, February 1997, p. 4. [http://www.rertr.anl.gov/METHODS/TM28.pdf].

7. W. F. Hughes and J. A. Brighton, *Shaum's Outline of Theory and Problems of Fluid Dynamics*, McGraw-Hill Book Company, New York, 1967, p. 29.

8. Sadik Kakac, Ramesh K. Shah, and Win Aung (Editors), *Handbook of Single-Phase Convective Heat Transfer*, John Wiley & Sons, New York, 1987, p. 4-146.

9. M. Troy, *WAPD-TH-340* (July 1957).
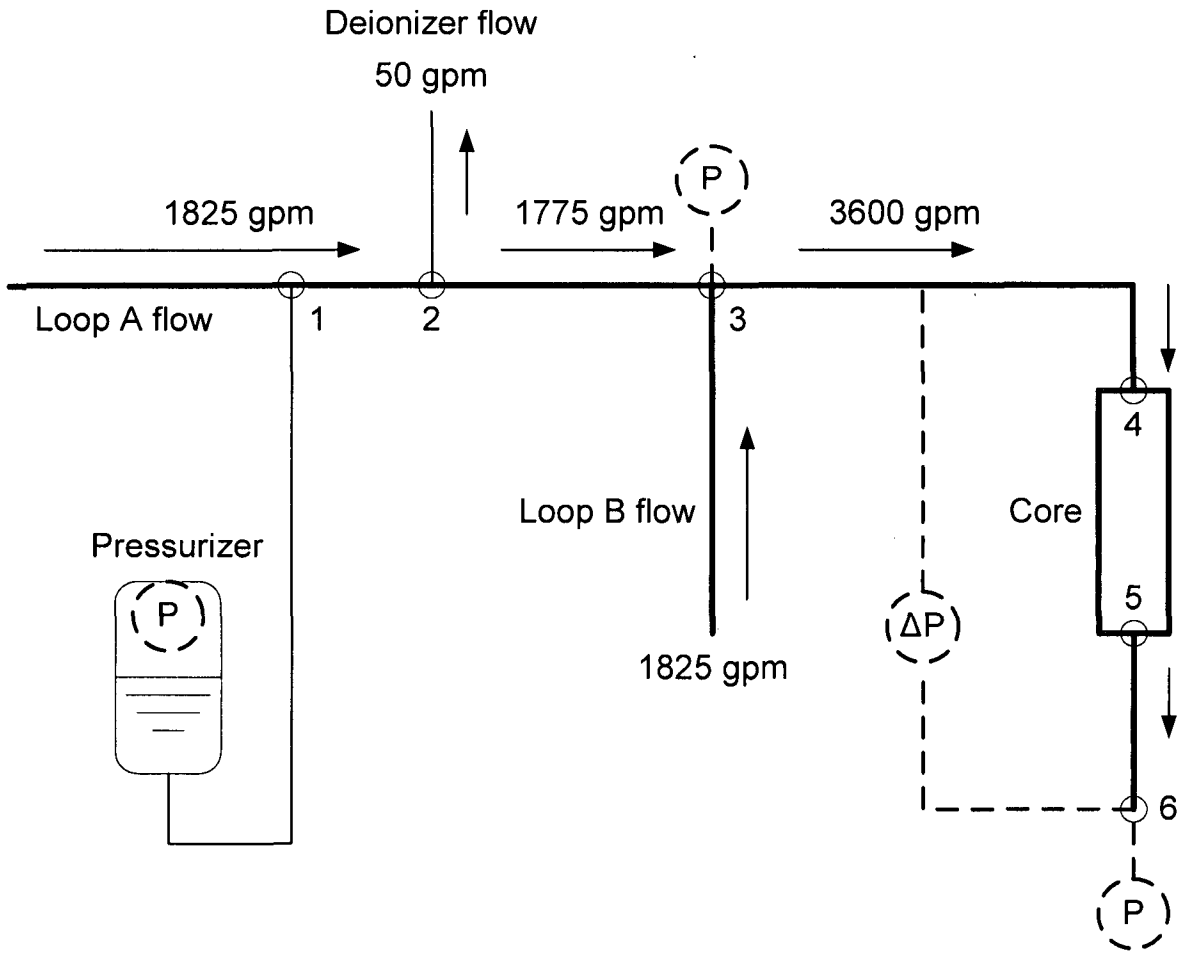
Figure 1 – Schematic Representation of the Reactor Core Inlet Piping

Table 1 – Power and Heat Flux Distribution Calculations for the Channel between Plates X1P01 and X1P02 (Core Power = 10 MW.)

A	B	C	D	E	F	G	H
	Heat Flux, W/cm²*		Plate Axial Peaking Factors		Weighted Average of Cols. D & E**	Col. F / ΣCol. F	Sum of Col. G from Level 1 to Current Level
Level	X1P01	X1P02	X1P01	X1P02			
1	50.9	41.5	0.393	0.405	0.863	0.0166	0.0166
2	54.0	41.6	0.417	0.406	0.893	0.0172	0.0338
3	61.6	49.2	0.476	0.480	1.036	0.0199	0.0537
4	73.6	57.3	0.568	0.559	1.222	0.0235	0.0772
5	86.6	67.6	0.669	0.659	1.440	0.0277	0.1049
6	99.4	78.3	0.768	0.764	1.660	0.0319	0.1368
7	112.8	87.3	0.871	0.852	1.868	0.0359	0.1727
8	124.1	98.1	0.959	0.957	2.076	0.0399	0.2126
9	137.8	108.3	1.064	1.056	2.298	0.0442	0.2568
10	148.7	118.6	1.149	1.157	2.498	0.0480	0.3048
11	158.9	124.9	1.227	1.219	2.651	0.0510	0.3558
12	167.9	133.5	1.296	1.302	2.814	0.0541	0.4099
13	173.7	137.5	1.342	1.341	2.907	0.0559	0.4658
14	**178.8**	140.8	**1.381**	1.373	2.984	0.0574	0.5232
15	178.7	**141.3**	1.380	**1.378**	2.989	0.0575	0.5806
16	178.7	141.0	1.380	1.375	2.986	0.0574	0.6380
17	172.5	138.2	1.332	1.348	2.902	0.0558	0.6938
18	167.8	133.0	1.296	1.298	2.810	0.0540	0.7478
19	158.8	126.4	1.227	1.233	2.664	0.0512	0.7991
20	147.8	116.9	1.141	1.141	2.472	0.0475	0.8466
21	135.5	107.1	1.046	1.045	2.266	0.0436	0.8902
22	121.4	95.2	0.938	0.929	2.023	0.0389	0.9291
23	107.6	86.3	0.831	0.842	1.811	0.0348	0.9639
24	110.5	90.5	0.853	0.883	1.878	0.0361	1.0000
Sum	3107.9	2460.5	24.0	24.0	52.01	1.0000	
Avg.	129.5	102.5	1.000	1.000			
Max.	178.8	141.3	1.381	1.378			
Plate Peaking Factor	2.215	1.754					
Azimuthal Peaking Factor	1.07	1.12					

*The heat fluxes in this Table are based on a core heat transfer area of 17.105 m², which is slightly smaller than the 17.108 m² value provided in section 3. Therefore, in this table the core average heat flux is 10 MW / 17.105 m² = 58.4621 W/cm². The extremely small discrepancy in core heat transfer area has absolutely no effect on the allowed values of reactor power because only the heat flux ratios in this table are used in the analysis.

**0.5 × (column D × product of its plate peaking and azimuthal peaking factors + column E × product of its plate peaking and azimuthal peaking factors)

**Table 2 – Sample Calculations of Local Heat Flux at Axial Level 18
for Limiting Reactor Power with All Factors Included
(To Be Compared with Bernath CHF)**

Reactor Power at Limiting Condition: 14.894 MW

Core Heat Transfer Area: 17.108 m^2

Fraction of Reactor Power Deposited in the Primary Loop: 0.93

Average Core Heat Flux: $0.93 \times \dfrac{14.894 \text{ MW}}{17.108 \text{ m}^2}$ = **0.8096 MW/m^2 = 80.96 W/cm^2**

Plate Axial Peaking Factor at Level 18
(Table 1, Column D, higher power plate of the two bounding the channel): **1.296**

Plate Average Peaking Factor (higher power plate of the two): 2.215
Plate Azimuthal Peaking Factor (higher power plate of the two): 1.07
Product of Plate Average and Azimuthal Peaking Factors (**Item A**): 2.215 × 1.07 = 2.3701

Engineering and Modeling Hot Channel Factors that Affect Local Heat Flux (**Item B**)
      Fuel Content (maximum overload for a plate): 1.03
      Maximum Fuel Meat Thickness / Average Thickness: 1.15
      Item B = 1.03 × 1.15

Product of Items A and B (**Item C**): 2.3701 × 1.03 × 1.15 = **2.807**

Additional Allowable Peaking Factor (**Item D**): 1.062

Overall Factor on Heat Flux without Axial Power Factor (Product of Items C and D = Product of Items A, B and D): 2.807 × 1.062 = **2.981**

Local Heat Flux at Axial Level 18: 0.8096 MW/m^2 × 1.296 × 2.981 = 3.13 MW/m^2 = 313 W/cm^2

Table 3 – Sample Calculations of Local Bulk Coolant Temperature at Axial Level 18 for Limiting Reactor Power with All Factors Included

Reactor Power at Limiting Condition: 14.894 MW
Reactor Volumetric Flow Rate: 3200 gpm = 0.2019 m³/s
Reactor and Channel Inlet Temperature: 155° F = **68.33° C**
Reactor Inlet Coolant Density: 978.4 kg/m³
Reactor Mass Flow Rate: 0.2019 m³/s × 978.4 kg/m³ = 197.5 kg/s
Coolant Specific Heat Capacity: 4.19 kJ/kg-C
Fraction of Reactor Power Deposited in the Primary Loop: 0.93

Core Temperature Rise: $0.93 \times \dfrac{14.894 \text{ MW}}{197.5 \text{ kg/s} \times 4.19 \text{ kJ/kg} - \text{C}} = $ **16.74° C**

Fraction of Channel Bulk Coolant Temperature Rise to the Exit of Level 18 (Table 1, Column H): **0.7478**

Plate Average Peaking Factors: 2.215 (Plate 1); 1.754 (Plate 2)
Plate Azimuthal Peaking Factors: 1.07 (Plate 1); 1.12 (Plate 2)
Combination of Plate Average and Azimuthal Peaking Factors (**Item A**):
    (2.215 × 1.07 + 1.754 × 1.12) / 2 = 2.167

Engineering and Modeling Hot Channel Factors That Affect Power (**Item B**)
    Fuel Content (maximum overload for a plate): 1.03
    Fuel Meat Thickness (tolerance factor on average fuel meat thickness): 1.03
    Item B = 1.03 × 1.03

Product of Items A and B (**Item C**): 2.167 × 1.03 × 1.03 = **2.299**

Additional Allowable Peaking Factor (**Item D**): 1.062

Overall Peaking Factor for Hot Channel (Product of Items C and D = Product of Items A, B and D): 2.299 × 1.062 = **2.442**

Engineering Hot Channel Factors That Affects Flow (Due to Channel Spacing Tolerance):
    Hot Channel Flow Area Factor: 0.90
    Hot Channel Factor for Velocity: 0.9108

    Both of the Above Combined: 0.90 × 0.9108 = **0.8197**

Maximum Bulk Coolant Temperature Rise to Channel Exit with All Hot Channel Factors Included: **16.74° C × 2.442 / 0.8197 = 49.87° C**

Bulk Coolant Temperature Rise to the Exit of Level 18: **0.7478 × 49.87° C = 37.29° C**

Bulk Coolant Temperature at the Exit of Level 18: 68.33° C + 37.29° C = 105.6° C

Table 4 – Sample Calculations of Local Bulk Coolant Velocity at Axial Level 18 for Limiting Reactor Power with All Factors Included

Reactor Volumetric Flow Rate (at Inlet Coolant Density): 3200 gpm = 0.2019 m^3/s

Reactor Core Total Coolant Flow Area: 0.3419 ft^2 = 0.03176 m^2

Average Coolant Velocity at Reactor Inlet (at Inlet Coolant Density):
0.2019 m^3/s / 0.03176 m^2 = **6.357 m/s**

Engineering Hot Channel Factor for Velocity (This is due to the hot channel having a thickness of 0.072 inches rather than the nominal value of 0.080 inches.): **0.9108**

Hot Channel Velocity at Channel Inlet: 6.357 m/s × 0.9108 = **5.790 m/s**

Reactor and Channel Inlet Temperature: 155° F = 68.3° C

Reactor Inlet Coolant Density: **978.4 kg/m^3**

Bulk Coolant Temperature at the Exit of Level 18 (See Table 3): 105.6° C

Reactor Coolant Density at the Exit of Level 18: **953.6 kg/m^3**

Hot Channel Velocity at the Exit of Level 18: 5.790 m/s × 978.4 kg/m^3 / 953.6 kg/m^3 = 5.941 m/s = 19.49 ft/s

Table 5 – Reference Hydraulic Conditions between the Pressurizer and the Core Exit Used in the Reference 2 Model

Component	ΔP_0, psi	Q_0, gpm*	T_0, °F	Frictional	Parallel Paths
1,2,3	3.259	1800	155	Yes	2
4	0.2689	1800	155	No	2
5 thru 10	4.08	3600	155	Yes	1
11	0.1977	3600	155	Yes	1
12	0.8980	3600	155	No	1
13	12.35	3600	165	Yes	in core

*Per Parallel Path

Table 6 – Reference Hydraulic Conditions between the Pressurizer and the Core Exit Used in the New Model

Component	ΔP_0, psi	Q_0, gpm	T_0, °F	Frictional
1	4.500	1825	120	No
2	0.0913	1825	120	Yes
3	0.2640	1775	120	No
4	3.3961	3600	120	Yes
5	1.1590	3600	120	Yes
6	0.0439	3600	120	No
7	0.7569	3600	120	No
8 (core)	13.8049	3608.3	128.68	Yes

Table 7 – New Model and Hot Channel Pressure Drops for 3200 gpm Core Flow, 155° F at the Core Inlet, 75 psia at the Pressurizer, and 14.894 MW Reactor Power (A negative value decreases the exit pressure.)

Item	New Model (Based on Core Avg.)	Hot Channel (Uses Eq. (10).)
Bernoulli Velocity	−2.897	−2.378
Friction	−10.394	−9.515
Gravity	+0.897	+0.887
Momentum Flux	0.	−0.176
Total	−12.394	−11.182

	A	B	C	D	E	F	G
1	Latest version as of June 6, 2011						
2	Step 1: Calculate reactor outlet pressure for specified power, flow rate, and inlet temperature.						
3							
4	New values based on benchmarked modeling.	Component	ΔP_0	Q_0	T_0	Frictional	
5	JCM 5/16/11	Group	psi	gpm	F		
6		1	4.500	1825	120	No	
7		2	0.0913	1825	120	Yes	
8		3	0.2640	1775	120	No	
9		4	3.3961	3600	120	Yes	
10		5	1.1590	3600	120	Yes	
11		6	0.0439	3600	120	No	
12		7	0.7569	3600	120	No	
13		8	13.8049	3608.3	128.68	Yes	
14							
15	1825 gpm $\Sigma \Delta P_0$ frictional at 120 F, psi	0.0913					
16	3600 gpm $\Sigma \Delta P_0$ frictional at 120 F, psi	4.5551					
17	1825 gpm $\Sigma \Delta P_0$ non-frictional at 120 F, psi	4.5000					
18	1775 gpm $\Sigma \Delta P_0$ non-frictional at 120 F, psi	0.2640					
19	3600 gpm $\Sigma \Delta P_0$ non-frictional at 120 F, psi	0.8008		Curve fit	Density	Viscosity	
20				a0	1004	1383	
21	1825 gpm frictional constant ($\Delta P / \Delta P_0$) before inlet	0.7579		a1	-0.1868	-26.04	
22	3600 gpm frictional constant ($\Delta P / \Delta P_0$) before inlet	0.7556		a2	-2.751E-03	0.2234	
23	1825 gpm non-frictional constant ($\Delta P / \Delta P0$) before inlet	0.7849		a3	0	-7.318E-04	
24	1775 gpm non-frictional constant ($\Delta P / \Delta P_0$) before inlet	0.7795					
25	3600 gpm non-frictional constant ($\Delta P / \Delta P_0$) before inlet	0.7822					
26							
27		reference conditions		core conditions			pressurizer
28		inlet	core avg.	inlet	average	outlet	pipe
29	Temp, F	120	128.68	155	170.06	185.13	85.00
30	Temp, C	48.9	53.7	68.3	76.7	85.1	29.4
31	density, kg/m^3	988.3	986.0	978.4	973.5	968.2	996.1
32	viscosity, micro Pa-s	558.4	515.5	413.3	369.8	334.0	791.3

Table 8 – Computer Spreadsheet for Determining Allowed Power (page 2 of 5)

	A	B	C	D
33				
34				
35	MPa per psi	6.894757E-03		
36	Cp, kJ/kg-k	4.19		
37				
38	Core Coolant Temp Rise, C, F	16.74	30.13	
39	Core Tavg, C, F	76.7	170.06	
40				
41	pressurizer low level SCRAM, inches	-16	MPa	Bar
42	static head: pressurizer to core exit (exit has lower press.), psi	-0.8673	-0.00598	-0.05980
43	1/2 * density * velocity^2 at fuel plate exit, psi, MPa, bar	2.897	0.01997	0.19971
44	flow area of 8" pipe at pressurizer attachment, ft^2	0.34741		
45	1/2 * density * velocity^2 at pressurizer attachment, psi	0.716	0.00494	0.04936
46	net pressure drop due to increase in velocity, psi, MPa, bar	2.181	0.01503	0.15035
47	Irrecoverable ΔP from Pressurizer to Core Inlet, psi, MPa, bar	7.875	0.05430	0.54297
48	frictional constant (ΔP / ΔP$_0$) for core	0.7529		
49	Irrecoverable ΔP across reactor core, psi, MPa, bar	10.394	0.0717	0.7166
50	Total ΔP from Pressurizer to Core Exit, psi, MPa, bar	21.32	0.1470	1.4698
51	Reactor Outlet Presssure, psia, MPa, bar	53.68	0.3701	3.7013
52				
53	total power, MW	14.894		
54	Inlet Temp, F, C	155	68.3	
55	Flow, gpm, m^3/s, ft^3/s	3200	0.2019	7.130
56	Pressurizer Press., psia, MPa, bar	75	0.5171	5.1711
57	Flow, kg/s	197.53		
58				

Table 8 – Computer Spreadsheet for Determining Allowed Power (page 3 of 5)

	A	B	C	D	E	F	G
59	Step 2: Adjust reactor power above until maximum ratio of local heat flux to local Bernath CHF is the desire value.						
60							
61	energy fraction generated in primary loop	0.93					
62	additional (allowable peaking) factor	1.062	greater than the week 58 peaking factors				
63	power factor for enthalpy rise without additional factor	2.299					
64	power factor for enthalpy rise with additional factor	2.442					
65	hot channel flow area factor	0.90	0.900 = 72 mils/80 mils; Used in calculating hot channel				
66	power factor for heat flux without axial factor or additional factor	2.807	bulk coolant temperature to exit				
67	power factor for heat flux without axial factor & with add'l factor	2.9814					
68	engineering hot channel factor for velocity	0.9108	Used in calculating: 1. hot channel bulk temperature rise				
69	heat transfer area, ft^2, m^2	184.15	17.108	to exit & 2. hot channel velcocity			
70	flow area, ft^2, m^2	0.3419	0.03176				
71	desire ratio of (max. heat flux)/CHF	0.499999					
72							
73	hot channel bulk temperature rise to exit, C	49.9					
74	hot channel exit temperature, C	118.2					
75	saturation temperature at core exit, C	140.9					
76							

Table 8 – Computer Spreadsheet for Determining Allowed Power (page 4 of 5)
(Columns I thru O are on page 5.)

	A	B	C	D	E	F	G	H
77	Axial Level	12	13	14	15	16	17	18
78	Plate Axial Peaking Factor	1.296	1.342	1.381	1.380	1.380	1.332	1.296
79	Fractional Bulk Temperature Rise	0.4099	0.4658	0.5232	0.5806	0.6380	0.6938	0.7478
80	overall power factor for heat flux	3.864	4.000	4.116	4.114	4.114	3.970	3.863094
81	hot channel heat flux, MW/m^2	3.129	3.239	3.332	3.331	3.331	3.215	3.128
82	Tbulk at allowed power, C	88.8	91.6	94.4	97.3	100.1	102.9	105.6
83	local density, kg/m^3	965.7	963.8	961.8	959.8	957.7	955.6	953.6
84	hot channel local V, ft/s	19.24	19.28	19.32	19.36	19.40	19.45	19.49
85								
86	De, m, ft, in	3.525E-03	0.011563	0.13876				
87	Di, m, ft, in	2.739E-02	0.089867	1.0784				
88	slope	697.3						
89	T_WBO, C	180.0	180.0	180.0	180.0	180.0	180.0	180.0
90	h_BO, pcu/hr-ft^2-C	14658	14684	14712	14741	14770	14800	14829
91	(Q/A)_BO [CHF], pcu/hr-ft^2	1337541	1298906	1259143	1219216	1179223	1140246	1102395
92	(Q/A)_BO [CHF], Btu/hr-ft^2	2407574	2338030	2266457	2194589	2122601	2052443	1984310
93	(Q/A)_BO [CHF], MW/m^2	7.590	7.371	7.145	6.918	6.691	6.470	6.256
94								
95	ratio of local heat flux to local CHF	0.412237	0.439389	0.466393	0.481426	0.497726	0.496832	0.499999
96	function heat flux ratio	1.161E-08						
97								
98	degrees of subcooling at core exit, C	22.66						
99								
100	minimum of (function heat flux ratio, subcooling at exit)	1.161E-08						

Table 8 – Computer Spreadsheet for Determining Allowed Power (page 5 of 5)
(Columns B thru H are on page 4.)

	A	I	J	K	L	M	N	O
77	Axial Level	19	20	21	22	23	24	
78	Plate Axial Peaking Factor	1.227	1.141	1.046	0.938	0.831	0.853	
79	Fractional Bulk Temperature Rise	0.7991	0.8466	0.8902	0.9291	0.9639	1.0000	
80	overall power factor for heat flux	3.657	3.402	3.119	2.795	2.477	2.543	
81	hot channel heat flux, MW/m^2	2.961	2.754	2.526	2.263	2.006	2.059	
82	Tbulk at allowed power, C	108.2	110.5	112.7	114.7	116.4	118.2	
83	local density, kg/m^3	951.6	949.7	948.0	946.4	945.0	943.5	
84	hot channel local V, ft/s	19.53	19.57	19.60	19.63	19.66	19.70	
85								
86	De, m, ft, in							
87	Di, m, ft, in							
88	slope							
89	T_WBO, C	179.9	179.9	179.9	179.9	179.9	179.9	
90	h_BO, pcu/hr-ft^2-C	14857	14884	14909	14932	14952	14974	
91	(Q/A)_BO [CHF], pcu/hr-ft^2	1066402	1032909	1002131	974583	949861	924174	
92	(Q/A)_BO [CHF], Btu/hr-ft^2	1919523	1859236	1803836	1754250	1709749	1663513	
93	(Q/A)_BO [CHF], MW/m^2	6.051	5.861	5.687	5.530	5.390	5.244	
94								maximum
95	ratio of local heat flux to local CHF	0.489302	0.469895	0.444123	0.409218	0.372150	0.392653	0.499999
96	function heat flux ratio					level of maximum		18
97								
98	degrees of subcooling at core exit, C							
99								
100	minimum of (function heat flux ratio, subcooling at exit)							

Nuclear Engineering Division
Argonne National Laboratory
9700 South Cass Avenue, Bldg. 208
Argonne, IL 60439-4842

www.anl.gov

Argonne
NATIONAL LABORATORY

June 15, 2011

TO: John G. Stevens

FROM: Earl E. Feldman

SUBJECT: Thermal-Hydraulic Effects of Reducing the Assumed Minimum Channel
Thickness of the University of Missouri Research Reactor HEU Core by 10 Mils[*]
to 62 Mils

SUMMARY

The reduction of the as-built minimum University of Missouri Research Reactor
(MURR) HEU core channel thickness from its 72 mil down to a minimum value to 62 mils
during use in the fuel cycle is analytically studied. The additional reduction is to account for
swelling due to fuel meat expansion from fuel burnup and clad thickening due to oxidation
buildup. If the channel thickness reduction is considered to occur at the core hot spot, the
allowed reactor power safety limit for steady-state operation would be decreased by 9% from
14.894 to 13.464 MW. However, the fuel meat void fraction of aluminide fuel causes the fuel
burnup to lead the accompanying reduction in channel size. This results in the heat fluxes of the
reduced channel being substantially less than those that existed when irradiation of the fuel
element was initiated. When this heat flux reduction is included in the analysis, this 62-mil end
of life minimum allowed channel thickness is predicted to reach its safety limit heat flux level
when the reactor power reaches 19.690 MW. This is 32% greater than the 14.894 MW reactor
power safety limit. Thus, the fuel elements with highest burnups and channel thicknesses
reduced to the minimum allowed are not among the most limiting ones.

1   BACKGROUND

In the manufacture of the University of Missouri Research Reactor (MURR) HEU
elements (i.e., assemblies) all fueled channels that are bounded by two fuel plates have a channel
thickness of 80±8 mils. The thermal hydraulic analysis in the MURR Safety Analysis Report
(SAR)[1] assumed that the thickness of the limiting channel was at the lower extreme of the
tolerance, 72 mils. The U.S. NRC review of the current MURR SAR, in the NRC Request for
Additional Information (RAI) Question 16.1, raised the issue of up to an additional 10-mil
reduction in a channel, which would reduce the minimum channel thickness to 62 mils. The
additional reduction would be a maximum allowance for swelling due to fuel meat expansion
from burnup and clad thickening due to oxidation buildup.

---

[*] 1 mil = 0.001 inches

The thermal limiting criteria for the MURR reactor during steady-state operation is based on avoiding both flow instability and critical heat flux. Reference 2 provides a detailed description of the model for defining the safety envelope for steady-state operation of the MURR reactor. This model is used below to address the issue of reduced channel thickness raised by the NRC in RAI Question 16.1.

Reference 2 includes a very detailed sample problem solution to promote clarity of the analytical model. Table 8 of Reference 2 shows the computer spreadsheet that was use for the sample problem to predict the allowed reactor power for a reactor inlet temperature of 155° F, pressure at the pressurizer of 75 psia, and total primary system flow rate of 3200 gpm. This combination of temperature, pressure, and flow rate corresponds to the Limiting Safety System Settings (LSSS) conditions as defined by the Technical Specifications for the MURR HEU core. The coolant channel chosen for analysis, channel 2 of element 1, is the innermost one bounded by two fuel plates and is the most limiting channel in the reactor. This sample problem with relatively minor changes to its input is used to address the issue of a reduced channel thickness.

2 ANALYSIS

The 10-mil maximum limit for reduction in channel thickness will cause a reduction in channel velocity and flow rate. The swelling and oxidation that causes reductions in channel thicknesses is a result of a substantial amount of irradiation and fuel burnup. Fuel plates in this condition produce substantially less power than they did when they were fresh fuel plates. The Reference 2 model will be used to assess the combined effects of an additional 10-mil reduction in channel spacing and the reduction in channel power production. First in section 2.1 the 10-mil reduction in channel spacing will be considered without the reduction in channel power production. Then in section 2.2 both effects will be considered together.

2.1 Effect of 10-Mil Reduction in Channel Thickness

The as-built channel thickness of all coolant channels in the HEU core that are bounded by two fuel plates is 80±8 mils. The assumed additional 10-mil maximum reduction in channel size due to oxidation and fuel swelling causes the minimum channel thickness to be 62 mils instead of 72 mils. Making the channel thinner reduces both its coolant velocity and its flow area. Both of these effects reduce its flow rate. Section 6 of Reference 2 considered an analogous situation where the limiting channel was assumed to have a thickness of 72 mils instead of its nominal thickness of 80 mils. The same analysis applies here with 62 mils used in place of 72 mils. The equations that were used are:

$$\frac{V_H}{V_N} = \left(\frac{D_H}{D_N}\right)^{\frac{1+\alpha}{2-\alpha}}$$

(1)

$$\frac{W_H}{W_N} = \frac{V_H \times A_H}{V_N \times A_N} = \frac{V_H}{V_N} \times \frac{A_H}{A_N} \qquad (2)$$

where V is velocity, D is hydraulic diameter, A is flow area, α is the exponent in the friction factor versus Reynolds number relationship, and subscripts H and N represent the hot and nominal channels, respectively. The friction, f, versus Reynolds number, Re, relationship is f $\propto$ $1/Re^{\alpha}$. Based on the Blasius formula for turbulent flow friction factor, f = $0.316/Re^{0.25}$, α is 0.25.

In Reference 2 the hot channel thickness is 72 mils, the nominal channel is 80 mils thick, D_H is 0.13876 inches, and D_N is 0.15828 inches. This value of D_H was obtained as 4 times the flow area divided by the wetted perimeter. The channel flow area is the product of the channel arc length along the average of the inner and outer radii and the channel thickness. The channel arc length is one-eighth the circumference of a circle reduced by both the thickness of two side plates (0.150 inches each) and the clearance between adjacent elements (0.04 inches). The nominal radii of the limiting channel analyzed in Reference 2 , channel 2 of element 1, are 2.820 and 2.900 inches, corresponding to a channel thickness of 0.080 inches. In Reference 2, for the hot channel, the inner radius was increased by 0.004 inches and the outer radius was decreased by 0.004 inches to account for the channel thickness tolerance of 0.008 inches, which reduced the channel thickness to 0.072 inches. Thus, for the Reference 2 hot channel, the flow area in inches^2 is:

$$\{2\,\pi\,[(2.820 + 2.900)/2] \,/\, 8 - (2 \times 0.150 + 0.04)\} \times 0.072 = 0.13725$$

and the wetted perimeters in inches is:

$$2\,\pi\,(2.820 + 2.900) \,/\, 8 - 2 \times (2 \times 0.150 + 0.04) + 2 \times 0.072 = 3.9565$$

The corresponding hydraulic diameter, D_e, in inches is 4 × 0.13725 / 3.9565 = 0.13876. For the 0.062-inch thick channel, the calculations for the flow area, wetted perimeter, and hydraulic diameter are the same as above except that 0.072 is replaced by 0.062. Thus, the new flow area, wetted perimeter, and hydraulic diameter are 0.11819 inches^2, 3.9365 inches, and 0.1201 inches, respectively.

For the current analysis the hot channel thickness is 62 mils instead of 72 mils and the nominal channel thickness is unchanged. The hot channel flow area factor, which is the area ratio A_H/A_N, is 62/80 = 0.7750. For the 62-mil channel, equation (1) yields V_H/V_N = $(0.1201/0.15828)^{(1+0.25)/(2-0.25)}$ = 0.8210. V_H/V_N is the engineering hot channel factor for velocity identified in the Reference 2 analysis. Equation (2) yields W_H/W_N = 0.8210 × 0.7750 = 0.6363.

The Reference 2 methodology also requires the value of the channel heated diameter (D_i), defined as the channel heated perimeter divided by π. D_i is the same for the reduced thickness channel as for the nominal thickness channel since thinning the channel does not change its heated perimeter.

In summary, changing the limiting channel thickness from 72 mils to 62 mils reduces A_H/A_N, which is the hot channel flow area factor from 0.90 to 0.775, V_H/V_N, which is the engineering hot channel factor for velocity, from 0.9108 to 0.8210, and the hydraulic diameter (De) from 0.13876 inches to 0.1201 inches. Substituting, the three new values, 0.775, 0.8210, and 0.1201, which are the hot channel flow area factor (cell B65), the engineering hot channel factor on velocity (cell B68), and De (cell D86), respectively into the Table 8 model of Reference 2 causes the predicted power at the LSSS conditions for pressure, temperature, flow rate to be reduced to 13.464 MW from 14.894 MW. This represents a 9% reduction in power. However, this analysis assumes that the heat flux distribution and peaking factors are the same as in the 72-mil channel analysis. A substantial amount of fuel burnup must occur before there is sufficient fuel swelling and clad surface oxidation to cause a 10-mil reduction in channel thickness. This burnup considerably reduces the element power. This is addressed in the next section.

2.2   Effect of the Increased Fuel Burnup That Causes the Reduction in Channel Thickness

Figure 1 and Table 1 show the plate axial peaking factors, which is the axial heat flux distribution, for the higher heat flux plate of the most limiting channel among the elements with high burnup. This plate is plate 1 of element 8, which has 142 MWd of burnup. The corresponding core configuration is for week 58, no-xenon (day 0), average CB rod height of 17 inches, and current (2008) graphite reflector. The plate peaking factor for this fuel plate, which is the plate average heat flux divided by the core average heat flux, is 1.5345. This is to be compared with its counterpart in Reference 2, which is 2.215. As in Reference 2, the limiting channel is the innermost channel in the fuel element that is bounded by two fuel plates. The power peaking factor was obtained from a MCNP code modeling of the MURR fuel cycle. The modeling to determine the power peaking factors only included the nominal coolant channel dimensions. If the hot channel #2 would have been modeled as narrower, it would have further reduced the power peaking due to the localized reduction in moderation.

The variation of heat flux along the azimuthal direction of each fuel plate is also taken into account. In the neutronics analysis the heated arc length along the azimuthal direction of each fuel plate is divided into a series of nine equal-radian arc length vertical strips. The average heat flux of each strip is calculated. The ratio of the highest of these nine averages to the plate-average heat flux is called the "azimuthal peaking factor". The plate axial peaking factors provided for each level in Table 1 are based on level-averaged heat fluxes rather than the level azimuthal maximum. The azimuthal peaking factor for the plate is 1.04, which is a lower value than for the limiting fuel plate in Reference 2 due to burnout of the hot stripe is greater than the average burnout.

In Reference 2 the bulk coolant temperature rise is based on a weighted average of the heat fluxes of the two fuel plates that bound the channel. This same approach was used in generating the values for the bulk coolant temperature in this analysis and given in Figure 1 and Table 1. These values for levels 12 through 24 of the axial power shape and fractional bulk temperature rise replace the ones shown in lines 78 and 79 of Table 8 of Reference 2 for the current analysis with high burnup.

The change in axial and azimuthal peaking factors affects two values in the Table 8 model of Reference 2. The "power factor for heat flux without axial factor or additional factor" (cell B66) was originally calculated in Table 2 of Reference 2 as $2.215 \times 1.07 \times 1.03 \times 1.15 = 2.807$. It now becomes $1.5345 \times 1.04 \times 1.03 \times 1.15 = 1.890$. The "power factor for enthalpy rise without additional factor" (cell B63) was originally calculated in Table 3 of Reference 2 as $2.167 \times 1.03 \times 1.03 = 2.299$, where the 2.167 was obtained as $(2.215 \times 1.07 + 1.754 \times 1.12) / 2 = 2.167$. As shown in Table 3 of Reference 2, the values 1.754 and 1.12 are the plate average peaking factor and the azimuthal peaking factor, respectively, of the other fuel plate bounding the channel in the Reference 2 analysis. For this analysis, since 2.167 is replaced with $1.5310 = (1.5345 \times 1.04 + 1.3702 \times 1.07)/2$ and $1.531 \times 1.03 \times 1.03 = 1.624$, 2.299 in cell B63 is replaced with 1.624.

When all of the new factors due to both the reduction in channel size and fuel burnup are in place in the Reference 2 model and the high burnup axial power shape is represented in lines 78 and 79, the 62-mil channel is predicted to reach its maximum safety limit power when the reactor power reaches 19.690 MW. This is 32% larger than the 14.894 MW reactor power safety limit of Reference 2.

3 DISCUSSION AND CONCLUSION

Steady-state operation of the MURR was analyzed in Reference 1. There is was found that for a reactor inlet temperature of 155° F, pressure at the pressurizer of 75 psia, and total primary system flow rate of 3200 gpm, which are the Limiting Safety System Settings (LSSS) conditions for these quantities, as defined by the reactor Technical Specifications, the allowed reactor power was 14.894 MW. This analysis assumed that the minimum spacing between adjacent fuel plates is 72 mils. The current analysis addresses the effect of reducing this minimum spacing due to burnup of the fuel an additional 10 mils to the minimum allowed 62 mils. First, the Reference 2 analysis was repeated with only the hot channel thickness reduced from 72 to 62 mils. This case corresponded to having the hot spot of the plate 1 in the highest heat flux location in the core of the fresh 0 MWd fuel element in the mixed burnup week 58 core occur with the narrow 62 mil channel of the 142 MWd end of life fuel element, which if possible would produce a 9% reduction in the safety limit power to 13.464 MW.

Since the reduction in hot channel thickness would be due to burnup, the current maximum burnup of a fuel element was assumed and the effect of burnup on the reactor heat flux distribution was also considered. The limiting channel was found to be channel 2 of element 8 instead of channel 2 of element 1. When the effect of fuel burnup on the heat flux of the most limiting 62 mil channel is included in the analysis, the 62-mil channel is predicted to reach its safety limit power when the reactor power reaches 19.690 MW. This is 32% larger than the 14.894 MW allowed reactor power safety limit of Reference 2. Therefore a 10 mil reduction in the limiting coolant channel to a minimum 62 mil channel over its burnup life time does not place a tighter restriction on the core safety limit. Thus, the fuel elements with higher burnups and reduced channel thicknesses are not among the most limiting ones.

REFERENCES:

1. University of Missouri Research Reactor Safety Analysis Report, Chapter 4, Reactor Description, submitted to the U.S. Nuclear Regulatory Commission in 2006.

2. Earl E. Feldman, Implementation of the Flow Instability Model for the University of Missouri Reactor (MURR) That is Based on the Bernath Critical Heat Flux Correlation, ANL-RERTR/TM-11-28, July 2011.
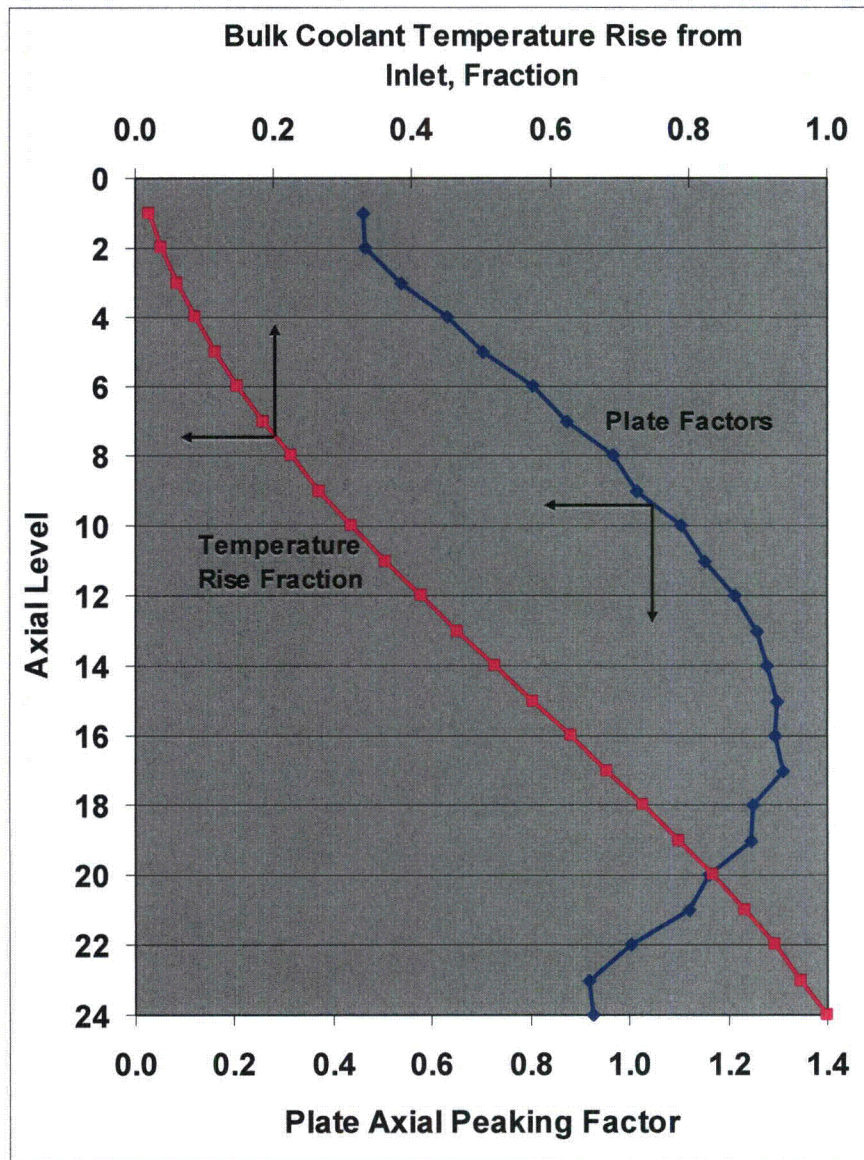
Figure 1 – Limiting Channel Plate Axial Peaking Factors and Coolant Temperature Rise Distribution

Table 1 – Limiting Channel Plate Axial Peaking Factors and Coolant Temperature Rise Distribution

Level	Plate Axial Peaking Factor	Fraction of Bulk Coolant Temperature Rise
1	0.461	0.0188
2	0.466	0.0377
3	0.537	0.0597
4	0.632	0.0857
5	0.705	0.1147
6	0.803	0.1478
7	0.872	0.1839
8	0.967	0.2241
9	1.016	0.2667
10	1.105	0.3132
11	1.152	0.3616
12	**1.214**	**0.4130**
13	**1.257**	**0.4658**
14	**1.278**	**0.5195**
15	**1.299**	**0.5743**
16	**1.297**	**0.6287**
17	**1.310***	**0.6833**
18	**1.250**	**0.7355**
19	**1.247**	**0.7875**
20	**1.162**	**0.8359**
21	**1.122**	**0.8821**
22	**1.002**	**0.9235**
23	**0.920**	**0.9614**
24	**0.925**	**1.0000**

*Maximum value